ELSEVIER

Advances in Water Resources 25 (2002) 293–303

Advances in Water Resources

www.elsevier.com/locate/advwatres

Transpiration dynamics of an Austrian Pine stand and its forest floor: identifying controlling conditions using artificial neural networks

Jasper A. Vrugt *, Willem Bouten, Stefan C. Dekker, Pieter A.D. Musters

Section Physical Geography, Institute for Biodiversity and Ecosystem Dynamics, University of Amsterdam, Nieuwe Achtergracht 166, Amsterdam 1018 WV, The Netherlands

Received 16 January 2001; received in revised form 19 November 2001; accepted 21 November 2001

Abstract

In this study, artificial neural network analyses (ANN) were used to identify the forcing environmental variables that are most significant in governing the transpiration rates of an Austrian Pine stand and its forest floor. Latent heat flux densities (Lh) of the Austrian Pine stand and its forest floor were separately measured using the eddy covariance technique. To assess the sensitivity of the ANNs to input information on the soil water status, the site calibrated soil hydrological model SWIF was used to compute average volumetric soil water contents of different depth intervals. Results show that forest floor transpiration dynamics can be adequately modelled using the global radiation reaching the forest floor and the topsoil water content (0–50 cm). The response functions of the total forest and forest floor showed a clear difference in sensitivity of latent heat fluxes to global radiation, air temperature and soil water content. Most significantly, results demonstrate that the presented ANN analysis is suited for assessing effective rooting depths from measured transpiration rates and soil water contents.

1. Introduction

The understanding of forest canopy–atmosphere exchange is of great importance to a variety of scientific issues, such as global and regional CO_2 and water balances, and the transport, dispersion and deposition of air borne pollutants [16]. The exchange of CO_2 and H_2O of the forest with the ambient atmosphere is largely controlled by the opening and closing of the stomata of the canopy. Therefore, the stomatal conductance of the canopy is generally considered to be a key element in predicting tree growth and water use at the stand scale.

In recent years, great effort is made in modelling instantaneous carbon and water fluxes at the stand scale [11,15]. Both top–down and bottom–up approaches are utilized to model short-term forest ecosystem fluxes. Several detailed physiological models use knowledge about photosynthetic and stomatal responses at the leaf level and scale these up to canopy level using sophisticated radiation interception models [6,35]. With these detailed models total forest evapotranspiration and carbon fluxes are predicted [34].

Despite the numerous studies concerning total forest evapotranspiration dynamics, not much attention has been paid to the mechanism controlling forest floor evapotranspiration dynamics [2]. The forest floor often accounts for a significant proportion of total forest evapotranspiration [13]. The partitioning of stand transpiration between trees and forest floor may vary depending on the soil water status [18,25] and the seasonal changes in leaf area of layers within the canopy. For an improved understanding of the magnitude and processes controlling forest floor evapotranspiration, more measurements are needed.

Physically based forest models are suitable tools to study the processes controlling the exchange of CO_2 and H_2O of the forest with the ambient atmosphere. A wide range of model types and variables is currently used, to predict forest ecosystem fluxes, indicating an incomplete knowledge of relationships between the forcing environmental variables and stomatal conductance of the canopy. For canopy evapotranspiration only, models range from the simple Priestley–Taylor formula [24] to simple biosphere [29,30], dual source [31,32] or multilevel models that take into account radiation distribution and turbulent exchange within the canopy [7,17]. In most of the canopy transpiration models the surface

* Corresponding author.
E-mail address: j.vrugt@science.uva.nl (J.A. Vrugt).

0309-1708/02/$ - see front matter
PII: S0309-1708(01)00061-6

conductance of the canopy is determined from a multiplicative-constraint function [10,33]. This function is usually specified in terms of maximum surface conductance reduced by bio-physical stress functions following Jarvis [10] and Stewart [33]. The parameters in these stress functions are either based on literature values or are estimated using an inverse modelling approach [3,33]. In this approach, the free parameters in the stress functions are optimised using a lumped error criterion containing the residuals between the measured and simulated transpiration fluxes.

Recently, Huntingford and Cox [9] and Van Wijk and Bouten [34] demonstrated that artificial neural networks (ANN) are excellent tools to model the stomatal conductance and evapotranspiration rates of forests, respectively. Compared to the physically based forest models, the ANN have an added skill in prediction because they succeed in modelling complex processes with a high precision without using an a priori model concept. In addition, ANNs can distinguish between relevant and non-relevant input variables, as the fit error of a network indicates how well output can be explained by input data [27]. The response curves of the different input variables, created by fixing other input variables at a certain value, also provides information about the sensitivity of the output to the driving input variables.

The purpose of the present study is to present a general ANN methodology which is suited to get hold on the forcing environmental variables and their functional form in governing the rate of transpiration for both the total forest and forest floor. As the ANN successively assimilates more and more forcing environmental variables, the fit error associated with the predictions decreases. This decrease in fit error emphasizes the relevancy of the extra information to model transpiration dynamics. In the ANN analyses, we are especially concerned with the sensitivity of the networks to information on the soil water status. The analyses are based on time series of latent heat flux densities of an Austrian Pine stand and from its forest floor using the eddy correlation covariance technique [36].

2. Materials and methods

2.1. Site description

The study was carried out within a forested area near Appelscha (52°58′N, 6°15′E), the Netherlands. This forested area, of about 4800 ha in size, is located in a driftsand area where vegetation mainly consists of large heather fields, Austrian and Scots Pine stands and bare driftsand areas. The measurements were located within a site of 0.11 ha within a larger homogenous stand of 54-year old Pines (*Pinus nigra* var. *nigra*) with a density of 640 trees ha^{-1}. A map of the plot is shown in Fig. 1. On average, Pine trees in this stand have an height of 10 m and a diameter at breast height of 22 cm. Temporal annual variation in Leaf Area Index (LAI) due to needle fall is between 1.4 and 2.4, resulting in a mean annual gap fraction of about 0.4. The understorey vegetation consists of mainly grass (*Deschampsia flexuosa* (L.) Trin., *Molinia caerulea* (L.) Moench.), moss (*Polytrigum* spec.) and heather (*Erica tetralix* L. and *Calluna vulgaris* (L.) Hull.). The water table at the lowest part of the driftsand dune in Fig. 1 usually ranges between −1.0 m at the beginning of spring and −3.0 m at the end of summer. The soil at the research site is classified as a Cambic Arenosol accordingly to the FAO classification [5]. Mean annual precipitation, interception and potential evapotranspiration are 850, 204 and 535 mm $year^{-1}$, respectively, while annual average temperature is 8.8 °C.

2.2. Transpiration measurements

In 1996 between days 180 and 243 and in 1998 between days 129 and 240 total forest latent heat flux densities were measured by the eddy covariance technique using 30 min covariance's of high-frequency (20 Hz) measurements of vertical wind speed (w; three-dimensional sonic solent anemometer, Gill Instruments, UK) and atmospheric water vapour density (Krypton KH_2O Hygrometer, Campbell Scientific, UK). Additionally, in 1998 forest floor latent heat latent heat flux densities were measured using the same equipment between days 128 and 240. The evaporation rate was calculated from $\overline{w'q'}$, where w' and q' are the fluctuations of the vertical wind velocity and the specific humidity around their mean value. The overbar signifies time average. Sensible heat fluxes were measured by the eddy covariance using $\overline{w'T'}$, where T is the air temperature measured by the sonic anemometer. Post data capture corrections included Webb et al. [36], 2 stage coordinate rotation and frequency response corrections [20]. The units were installed at, respectively, 12 m (tower), about 2 m above adjacent Pine trees, and 3.5 m above the forest floor. The eddy correlation units were pointed into the prevailing wind direction.

Assuming horizontal homogeneity and neglecting the energy used in photosynthesis, the energy budget of a forest stand or forest floor, can be expressed as

$$R_n - S - G = H + \lambda E, \tag{1}$$

where R_n is the net radiation, G is the soil heat flux, S is the rate of heat storage, H is the sensible heat flux and λE is the latent heat flux, all of which have units in W m^{-2}. Ideally, the available energy $(R_n - S - G)$ should be balanced by the sum of the eddy fluxes, $H + \lambda E$. The heat storage and soil heat flux were estimated using measured temperature profiles within the canopy and mineral soil, respectively. Fig. 2 shows a

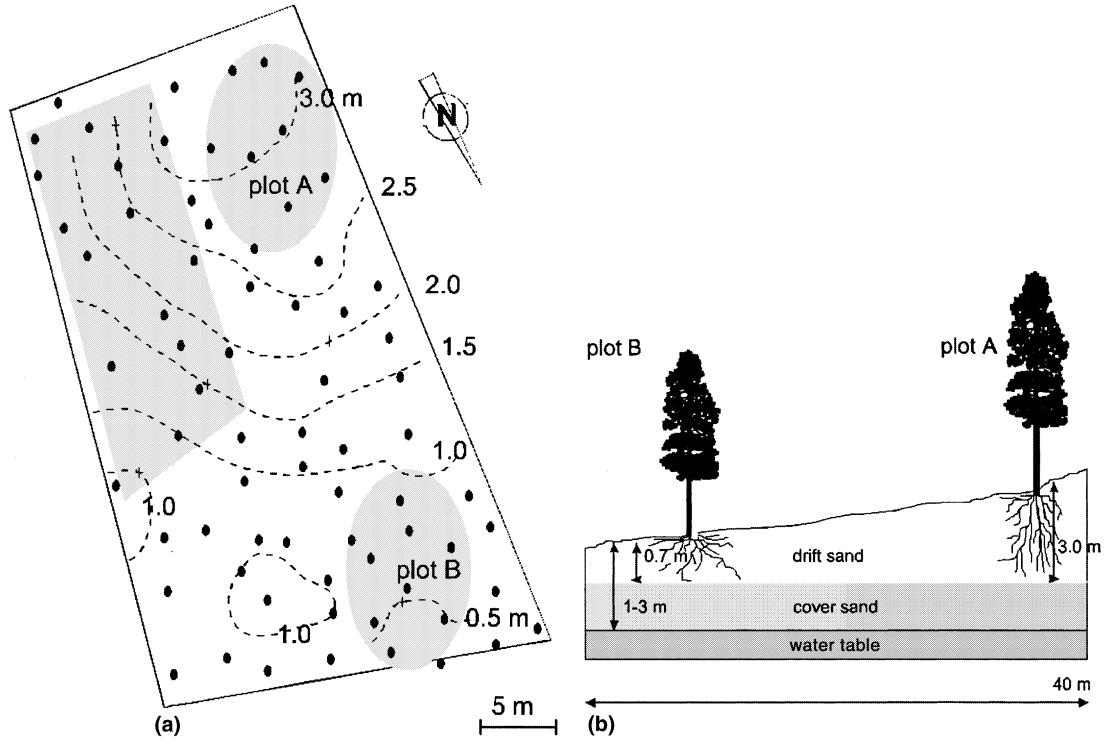

Fig. 1. (a) Map of the monitoring location. Variations in the depth of the driftsand layer are marked with dotted contour lines in (*m*), trees are marked with a '•'. (b) Schematic side view of the field site.

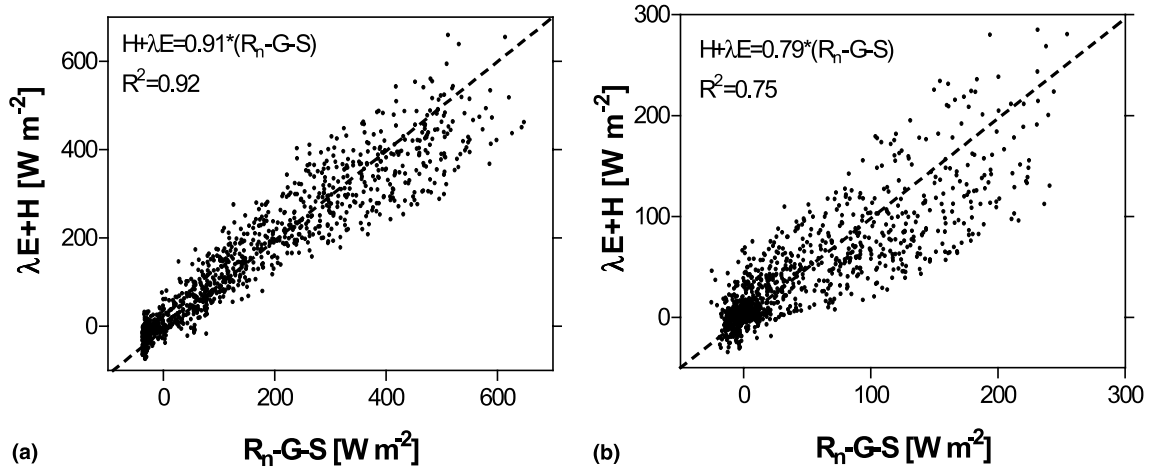

Fig. 2. Scatter plot of sum of the eddy fluxes against available energy: (a) total forest; (b) forest floor. The dashed line is the 1:1 line.

scatter plot of the sum of the eddy fluxes ($H + \lambda E$) against the available energy ($R_n - G - S$). A distinction is made between the eddy fluxes and available energy of the total forest (2*a*) and eddy fluxes and available energy within the stand (2*b*). According to Fig. 2 the overall closure of the energy balance for both the forest floor and the total forest is satisfactory. Nearly identical results with respect to the validity of eddy flux measurements within an Pine stand were recently obtained by Lamaud et al. [14]. The closure of the energy balance for the total Austrian Pine stand is comparable to the results of Kelliher et al. [13] in a Siberian Pine stand. At high available energy the sum of eddy fluxes is slightly lower. On daily basis, the ratio between the daytime total eddy flux of sensible and latent heat to the available energy of the forest floor had an average value of 0.82.

2.3. Environmental measurements total forest

Air temperature (T) and vapour pressure deficit (VPD) were measured at 15 m height in a tower with

Grant Delta-T ventilated psychrometers having a specified accuracy of 0.06 K. Wind speed (u) was also measured at 15 m height with a Vector A101M anemometer equipped with a 3-cup rotor (Vector R60). This combination provided a starting speed of about 0.15 m s^{-1}. Additionally, net radiation was measured in the same tower at 15 m height with a Fritschen (REBS, USA) $Q*7.1$ net radiometer with hard shield, whereas global radiation was measured at the same height with a Kipp pyranometer (Delft, The Netherlands).

2.4. Environmental measurements within Austrian Pine stand

To study the processes that control forest floor transpiration dynamics, additional environmental measurements were performed within the Austrian Pine stand. Again, air temperature (T) and vapour pressure deficit (VPD) were measured at 2 m above the forest floor with Grant Delta-T ventilated psychrometers. Wind speed (u) was also measured at 2 m height above the forest floor with a Vector A101M anemometer equipped with a 3-cup rotor (Vector R60).

It is clear that where values of spatially average net irradiance within the Pine stand are required for shorter time intervals than a day that the use of a stationary net radiometer is not adequate [2]. Therefore, the net radiation reaching the FF was measured with a Q-7 (Campbell Scientific, UK) net radiometer, implemented on a travelling tram system. This tram travelled with a speed of approximately 2.5 m min^{-1} over a distance of 7.5 m. The tram automatically turned by entering the end of the travelling path. Measurements were performed 10 times a second and transmitted to a data logger with receiver. A preliminary analyses of the data demonstrated that the measured half-hourly values of net radiation within the Austrian Pine stand showed an excellent relation with measured net radiation dynamics above the Pine stand ($R^2 = 0.96$).

The global radiation reaching the forest floor was deduced from the measured global radiation above the Austrian Pine trees multiplied with the complementary part of the gap fraction of the stand. This approach seemed most appropriate as measured global radiation dynamics within forest exhibited a highly dynamic sun-shatter pattern being associated with the position of the Pine trees in relation to the sun. All the environmental measurements within and above forest were stored as half-hourly values with a CR10 datalogger. Soil water contents within the Pine stand were measured with a 90 channel automated TDR system [8]. A detailed description of the TDR system is given by Musters et al. [22] and so will not be repeated here.

2.5. Soil water content

The soil water availability influences the fraction of the available energy that is used for transpiration. As we are especially concerned with the sensitivity of the ANN to input on the soil water status, the site calibrated soil hydrological model SWIF was used to compute average soil water contents at different depths in the soil. This model simulates unsaturated soil water flow by numerically solving the one-dimensional Richards' equation in which root water uptake is treated as a sink term. The SWIF model was calibrated on measurements of volumetric soil water content during 1995 and 1996 by Musters et al. [22]. The model was used to compute average volumetric soil water contents at depth intervals, 0–20, 0–50, 0–100, 0–200 and 0–300 cm, and to interpolate in time. These depth intervals were chosen based on the earlier reported work of Musters and Bouten [21], who determined rooting depths of the Austrian Pine stand by inverse modelling the spatial variability in measured soil water contents. Fig. 3 shows simulated and measured water contents at two different depths in the soil profile between days 60 and 260 in 1998. Although some mismatches are found, simulated water contents agree well with measured ones. Mea-

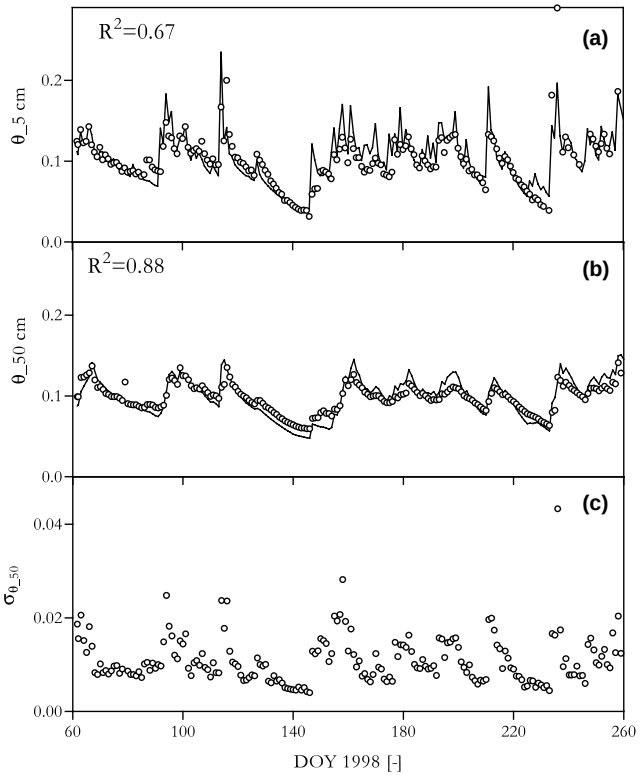

Fig. 3. Soil water dynamics for the monitoring plot: (a) measured (symbol '○') and simulated volumetric soil water contents ('——') at 5 cm depth; (b) measured and simulated volumetric soil water contents at 50 cm depth; (c) standard deviation σ in measured volumetric soil water contents at 50 cm depth.

sured spatial variations in water contents are relatively high, and as a result almost all of the mismatches can be attributed to the variability of measured water contents.

2.6. Artificial neural networks

Artificial neural networks (ANN) can be considered as black-box models that are capable of recognising and mimicking complex relations between input and output variables [27]. The major advantage of an ANN is its ability to represent the non-linearity by means of smaller number of parameters and to learn from examples. ANN learn through an iterative procedure known as training, which in turn adjusts the parameters (weights) of the network [26]. In the present study a multi-layer feed-forward back-propagation network is selected because of its versatility in function approximation [23]. Fig. 4 shows a schematic view of the three-layer back-propagation network that we used. These networks calculate the output $Y(t)$ at time t from the instantaneous input variables $X_i(t)$ with a complex mathematical network of connective nodes or 'neurons'. A sigmoid transfer function was used for the neurons in the hidden layer and a linear transfer function for the output layer, since this combination of transfer functions can represent any functional relationship between input and output variables. The weights and biases in the NN were obtained in an iterative calibration procedure based on the Levenberg–Marquardt algorithm [19]. A neural network obtained in the calibration procedure should always be tested on independent data. Usually this is done by calibrating the neural network on one part of a data set and subsequently testing the network on another part. We followed this approach and also estimated uncertainty in the artificial neural network predictions by combining multiple calibrations and testing runs with the bootstrap method [4]. Bootstrapping simulates different realisations by repeated random resampling with replacement of the original data set of size N to yield B bootstrap data sets. Each bootstrap data set contains somewhat different data, which results in B neural network models. We used a value of B of 30. By calculating averages and standard deviations of B testing results, one obtains robust values of the predictions and associated uncertainty estimates for independent data [28]. As we tried to keep the ANN as simple as possible, we built ANN with two hidden nodes in the hidden layer. Increasing the number of hidden nodes did not improve the model fit.

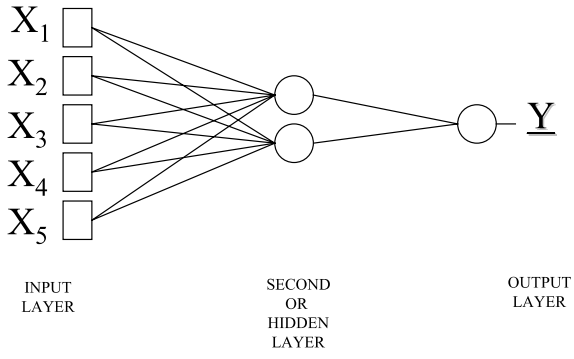

Fig. 4. Schematic view of a three-layer back-propagation artificial neural network with 5 input variables.

For both the total Austrian Pine stand and its forest floor we build 61 ANN models, with different combinations of input variables to determine the most relevant input variables for modelling the transpiration rates. These input variables included, global radiation (R), temperature (T), wind speed (u), vapour pressure deficit (VPD), time of year (t_s) and the average soil water content of different depth intervals ($\theta_{0-20}, \theta_{0-50}, \theta_{0-100}$, θ_{0-200} and θ_{0-300}) as calculated using the SWIF model. The input variable t_s was presented as the Julian number of day and was included to simulate the LAI dependency of the water use of the total forest and forest floor.

For the final data set, only those measurements were selected with real forest floor or total ecosystem transpiration. For this purpose measurements within 5 h after a rain event were omitted from the data set to avoid the process of interception evaporation. Additionally, condensation fluxes ($LE < 0$) were eliminated from the data set to concentrate on processes being associated with transpiration. Finally, we obtained a data set with 1280 half-hourly measurements for the total forest and 1185 measurements within forest. Table 1 presents some statistics of the micrometeoro-

Table 1
Some general statistics of the measurements of global radiation (Q), specific humidity deficit (δq), air temperature (T), latent heat flux (λE) and sensible heat flux (H) for the total forest and for the forest floor

	Total forest					Forest floor				
	Q (W m^{-2})	δq (mbar)	T (°C)	λE (W m^{-2})	H (W m^{-2})	Q (W m^{-2})	δq (mbar)	T (°C)	λE (W m^{-2})	H (W m^{-2})
Mean	220.7	7.2	17.7	66.5	70.5	94.6	7.8	14.4	26.0	13.4
Min	2.0	0.0	5.3	0.0	−89.8	0.0	0.0	0.9	0.0	−49.0
Max	866.3	29.4	30.2	220.8	400.4	346.5	29.3	29.0	116.0	169.3

logical measurements of the final data set. The analyses with the artificial neural networks now aimed at selecting those environmental variables that control total forest and forest floor latent heat flux densities. For this, the performance of ANN models with different input combinations of environmental variables were compared in terms of misfit with measured transpiration rates.

3. Results and discussion

The results with the ANN analyses are discussed in three different stages. Stage 1 illustrates the performance of the various ANN models. In this section we are especially concerned with identifying those forcing environmental variables, which are most significant in governing the transpiration rates of the Austrian Pine stand and its forest floor. Subsequently, in stage 2 these results are used to choose for a single best ANN model, taking into account the number of free parameters and the corresponding misfit measure. Finally in stage 3 we present the network responses to the forcing environmental variables and make inferences regarding the contribution of forest floor transpiration to total stand transpiration.

3.1. Performance of the ANNs

The average test results of 61 bootstrap ANNs with the most important input variable combinations are shown in Table 2. A distinction is made between ANN predicting the measured latent heat fluxes of the total Austrian Pine stand and ANN predicting the measured latent heat fluxes of its forest floor. As becomes clear from Table 2, the global radiation is an important input variable for modelling the latent heat fluxes of both the total forest and its forest floor. Additionally, including generally accepted driving forces for transpiration like air temperature, T, vapour pressure deficit, VPD, and wind speed, u, only slightly improves the fit error of the ANN. Moreover, these input features may affect transpiration rates during certain moments, but apparently these moments occur rarely within the period of measurements. Furthermore, as some of the input variables like temperature, VPD and global radiation are correlated, there is hardly any additional information in Temperature and VPD for modelling latent heat fluxes.

The dependency of the performance of the ANN for information on the soil water status is confirmed by differences in fit error, as caused by providing different average soil water contents at different depth intervals as input to the ANN. This sensitivity for input on the soil waters status is in agreement with the low water holding capacity of this sandy soil, which favours easily development of water stress, thus influencing transpiration rates. Fig. 5 illustrates how the misfit of the ANN is related to the average soil water content provided to the network for both the total forest as its forest floor. The error bars depict the uncertainty in RMSE values being associated with the 30 bootstrap networks. For brevity we only displayed graphical results for ANNs T23 up to T27. Fig. 5 and Table 2 demonstrate that the average

Table 2
Standard deviation between measured and predicted latent heat (Lh) fluxes for different ANN models for the total forest and the forest floor

Model	Pars.	Input	Total forest					Forest floor				
			θ_{0-20}	θ_{0-50}	θ_{0-100}	θ_{0-200}	θ_{0-300}	θ_{0-20}	θ_{0-50}	θ_{0-100}	θ_{0-200}	θ_{0-3}
T1	7	R	23.7					12.6				
T2	7	VPD	43.1					18.1				
T3	7	T	43.6					18.7				
T4	9	R, θ	24.1	23.7	22.9	22.2	22.6	11.8	11.3	11.8	12.1	12.2
T9	7	t_s	54.5					25.2				
T10	9	R, VPD	22.9					12.3				
T11	9	R, T	24.2					11.7				
T12–T16	9	VPD, θ	42.5	43.2	42.2	40.2	41.6	17.5	17.5	17.5	17.5	17.8
T17	9	VPD, T	43.4					16.8				
T18–T22	11	R, VPD, θ	22.1	22.6	22.0	21.6	21.9	11.3	11.3	11.8	11.6	11.6
T23–T27	11	R, T, θ	23.4	23.3	22.0	21.1	22.1	11.8	11.2	11.7	11.7	11.7
T28	11	R, VPD, T	23.3					11.9				
T29	11	R, VPD, u	21.6					12.0				
T30	11	VPD, T, u	37.0					17.0				
T31–T35	13	R, VPD, θ, u	21.8	21.6	21.0	21.0	21.8	11.3	11.0	11.5	11.2	11.1
T36–T40	13	R, VPD, T, θ	22.8	22.6	22.1	21.2	21.4	11.3	11.1	11.7	11.6	11.4
T41	13	R, VPD, T, u	22.2					11.3				
T42–T46	13	VPD, T, θ, u	35.7	37.5	36.7	37.1	34.9	17.6	17.1	17.4	17.3	17.3
T47–T51	15	R, VPD, T, θ, u	22.8	21.6	21.5	21.2	21.7	11.0	10.8	11.0	11.0	10.9
T52–T56	15	R, VPD, T, θ, t_s	22.8	22.1	22.8	20.1	20.7	11.8	11.0	11.6	11.9	11.2
T57–T61	17	R, VPD, T, θ, u, t_s	23.0	21.7	21.5	20.1	20.2	11.2	10.7	11.1	11.1	11.4

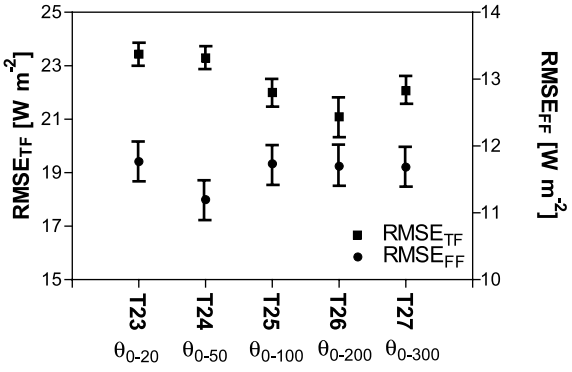

Fig. 5. Characteristic dependency of fit error of ANN network models (T23–T27) as function of the average volumetric soil water contents provided to the network. The left y-axis corresponds to the prediction error of the ANN models of the total forest.

soil water content between 0 and 200 cm, contains most information for modelling the latent heat fluxes of the total forest, whereas this depth interval is between 0 and 50 cm for the forest floor. These results agree extremely well with results by Musters and Bouten [21], who found from inverse modelling of spatial variability in measured soil water contents that rooting depths of the Austrian Pine trees ranged between 0.8 and 3.2 m. Additional root observations from a trench of 50 m long and 2.5 m deep at 50 m from the monitoring plot, confirmed that the rooting depth of the understorey generally ranged between 0 and 30 cm. This suggests that the presented ANN analyses is suited to assess effective rooting depths from measured latent heat fluxes and volumetric soil water contents.

The number of hidden neurons in a network is an indication of the complexity of the modelled process [27]. Latent heat fluxes were modelled with only two hidden neurons, suggesting a remarkable simplicity. Most likely, this low number of parameters results from the strong correlation between global radiation, R, and the latent heat flux of the total forest and forest floor ($R^2 = 0.82$ and 0.78, respectively).

3.2. Model selection

With recourse to the quality of the fit only, the most complex ANN models being associated with 15–17 parameters seem most appropriate. However, as a correct model selection should reflect a compromise between the number of free parameters and the corresponding misfit, we selected model T26 for the total forest and model T24 for the forest floor. Both ANN models use global radiation, temperature and soil water content, either averaged over 0–50 or 0–200 cm, as input variables. ANNs with more input variables (T31–T61) and thus more free parameters (15–17) perform approximately comparable. Fig. 6 presents a scatter plot between measured and modelled latent heat fluxes, using ANN model T26 for the forest floor (6*b*) and T24 for the total forest (6*b*). In general, modelled latent heat fluxes match the measured ones, i.e. no striking deviations from the 1:1 line are found. The standard deviation between the measured and predicted Lh-fluxes of 21.1 W m^{-2} for model T26 for the total forest is comparable to the results of Van Wijk and Bouten 34, who analysed water and carbon fluxes above a range of European coniferous forest with ANNs. Hence, the lower RMSE of ANN describing transpiration fluxes of the forest floor (11.2 W m^{-2}) as compared to ANN describing Lh-fluxes of the total forest (21.1 W m^{-2}) is primary due to the lower transpiration fluxes originating from the forest floor. The cut-off of modelled latent heat fluxes by the ANNs, which is clearly visible in Fig. 6 are due to artefacts in the transfer functions used in the network and the relatively large measurement errors of the highest eddy fluxes [9,34]. The sigmoid shape of the transfer functions in the hidden layer, do not allow any differentiation in network response a the upper bound, resulting in a clear cut-off of modelled Lh-fluxes, so evidently present in Fig. 6. Although not presented here, replacement of global by net radiation as input to the ANN did not improve the overall model fit.

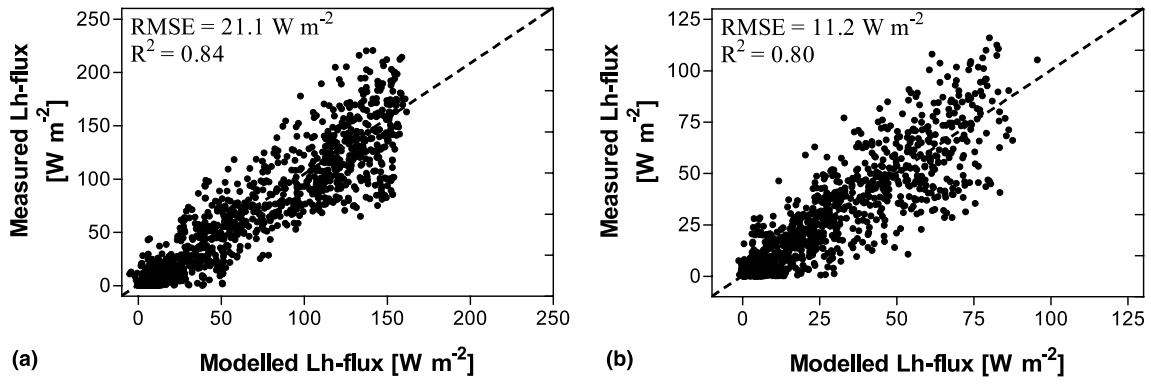

Fig. 6. Scatter plot of measured against simulated latent heat fluxes for the total forest and forest floor.

3.3. Functional form response functions

In Fig. 7 we present the functional form of the response functions of model T1, T7 and T26 for the total forest and model T1, T5 and T24 for the forest floor. For ANN models, which use more than one input variable, these response functions were created by varying one input variable within its measured range (displayed on the x-axis) in the ANN, while keeping the other input information fixed at its mean value. As ex-

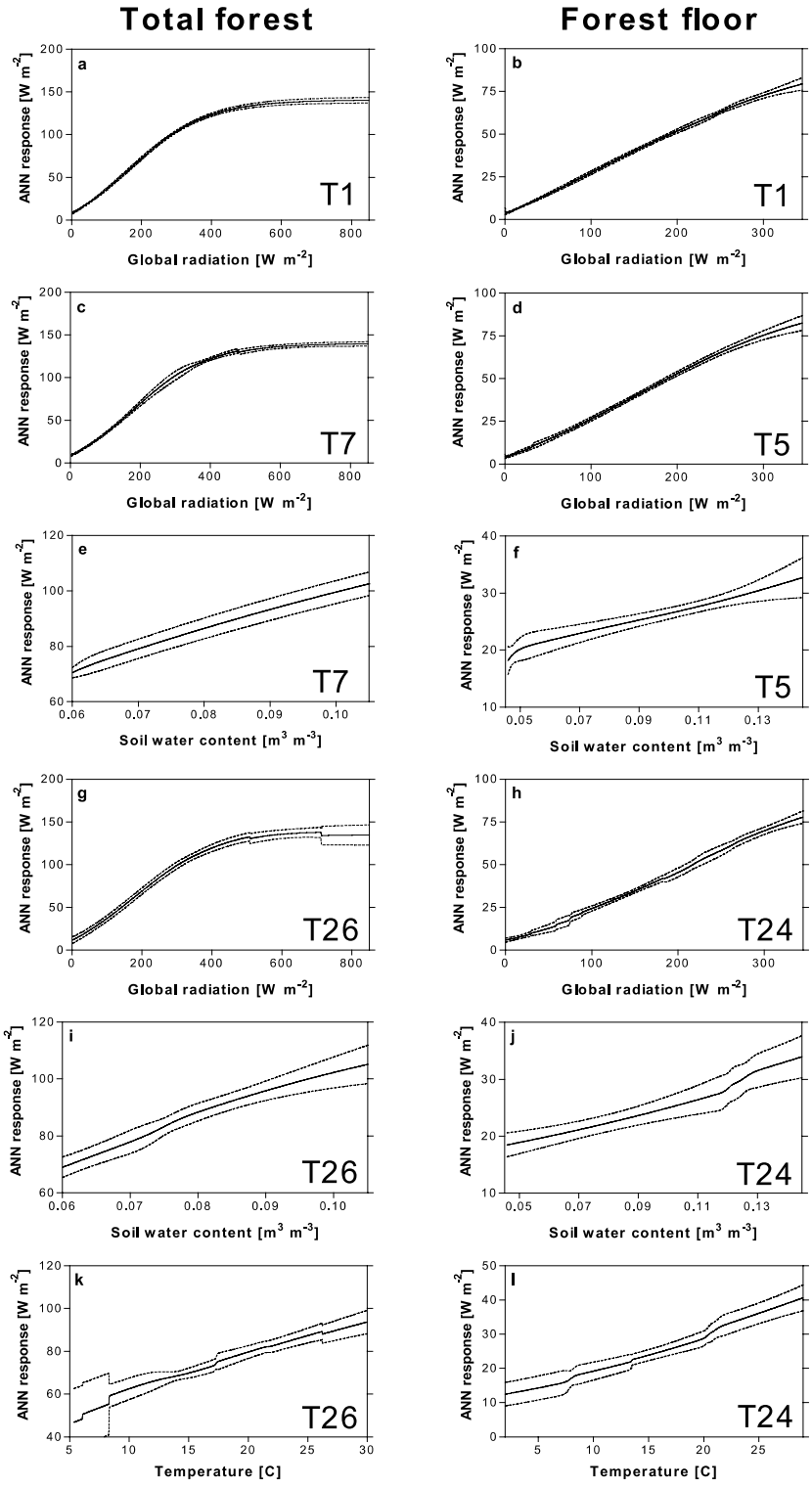

Fig. 7. Functional form of response functions for ANN models T1, T7 and T26 for the total forest stand and T1, T5 and T24 for the forest floor. For more explanation see text.

trapolation of ANNs beyond the range of measurements present in the calibration set is questionable, we only showed the ANN responses to the measured range of forcing environmental conditions.

The network response to global radiation is convex for the total forest, whereas an almost linear response is found for the forest floor. Additionally, the response of the ANN to global radiation is almost identical for the models T1, T5 and T24 for the forest floor and T1, T7 and T26 for the total forest. This primarily indicates that correlation between the input variables is typically low. The functional form of the response of the total forest resemblances the commonly used Stewart–Jarvis response functions to global radiation as was also found by Huntingford and Cox [9]. The relatively small standard deviation of the 30 ANN bootstrap models, as indicated by the dashed lines, shows the clear potential of using measured latent heat fluxes to identify the transpiration response to global radiation. Furthermore, within the range of global radiation reaching the forest floor, the functional form of the response of the ANN to global radiation is almost identical for both the total forest and forest floor.

Fig. 7(k) and (l) show that variations in air temperature have only a limited effect on the response of the ANN, as compared to the global radiation response. The relatively large uncertainty of the temperature response of network T26 for the total forest at low temperatures is associated with a relatively small number of Lh-flux measurements. Additionally, the smaller variability in average soil water contents of the 0–200 depth interval (Fig. 7(e) and (i)) as opposed to the 0–50 depth interval (Fig. 7(f) and (j)) is caused by the use of a larger depth interval, which buffers the variability in soil water contents. Fig. 7(i) and (j) clearly demonstrate that the network response to the average volumetric soil water content is approximately linear, for both the total Austrian Pine stand and its forest floor. A similar kind of linearity has also been reported by Kelliher et al. [12] for grasslands and forest. Moreover, an almost identical shape and uncertainty in response of the ANN to soil water content is found for models T7 and T26 of the total forest and model T5 and T24 for the forest floor. Using a linear approximation, a decline of 0.01 $m^3\ m^{-3}$ in soil water content leads to a decrease in ANN response with 8.75 $W\ m^{-2}$ for the total forest and 1.75 $W\ m^{-2}$ for its forest floor. Combining these results with the average latent heat fluxes of the total forest (66.5 $W\ m^{-2}$) and forest floor (26.0 $W\ m^{-2}$), as presented in Table 1, one can conclude that, as percentage, the transpiration rate of the Austrian Pine trees is more sensitive to the soil water content than its forest floor or understorey.

Finally, in Fig. 8 we present the modelled half-hourly transpiration rates of the total Austrian Pine stand and its forest floor for two periods using the calibrated ANN model T26 and T24, respectively. On average, forest floor transpiration accounts for 38% of total forest transpiration. Recently, Kelliher et al. [13] obtained ratios between 33% and 92% on daily contribution of understorey evapotranspiration on dry days in a Siberian Pine forest. In a *Pinus banksiana* L. forest with a comparable tree canopy leaf area of 2, Baldocchi et al. [1] concluded that this percentage was between 10% and 40% (mean of 25%).

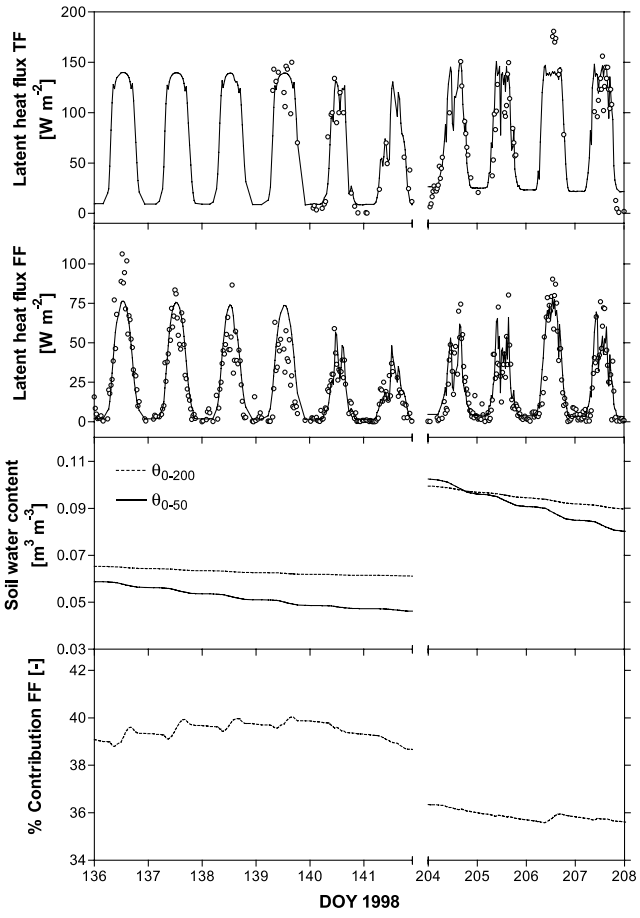

Fig. 8. Measured (symbol '○') and modelled latent heat fluxes ('——') for two periods in 1998. Also displayed are the average soil water contents of the 0–50 and 0–200 depth interval, and the contribution of forest floor evapotranspiration to total stand evapotranspiration.

4. Conclusions

In this paper, we used artificial neural networks (ANN) analyses to detect the processes controlling the transpiration dynamics of an Austrian Pine stand and its forest floor. A major advantage of ANNs for modelling transpiration rates is their flexibility and ability to model the response to environmental driving forces, without using any deterministic relation. The site calibrated soil hydrological model SWIF was used to assess the sensitivity of the ANNs to input information on the soil water status.

The ANN analyses revealed that transpiration rates of the total Austrian Pine stand can adequately be modelled (RMSE = 21.1 W m^{-2}; $R^2 = 0.84$) using the global radiation, the air temperature and the average water content between 0 and 200 cm in the soil. Transpiration rates of the forest floor can be adequately modelled (RMSE = 11.2 W m^{-2}; $R^2 = 0.80$) using the global radiation reaching the forest floor, the air temperature above the forest floor and the average soil water content between 0 and 50 cm in the soil. Results demonstrated that the presented ANN methodology is suited to assess effective rooting depths from measured latent heat fluxes and soil water contents.

The functional forms of the response functions of the total forest and forest floor showed different sensitivities of the total forest and forest floor transpiration fluxes to these environmental conditions. Within the range of global radiation reaching the forest floor, the functional shape of the response function of the ANN to global radiation is almost identical for both the total forest as its forest floor. However, outside this range, at higher amounts of global radiation, the total forest shows a convex response. In both cases, the network response to the average soil water content was approximately linear. Moreover, transpiration rates of the Austrian Pine trees were more sensitive to the soil water content than its forest floor or understorey. The contribution of forest floor transpiration to total stand transpiration generally ranged between 35% and 40% on daily basis. This contribution increased during periods of drought.

Acknowledgements

The authors would like to acknowledge E. Sabajo of the University of Amsterdam for developing the travelling tram system, M.G. Schaap of the Salinity Lab for providing the combined ANN-bootstrapping software and A.J. Dolman of the Staring Centrum for making use of one eddy correlation unit. The Earth Life Sciences and Research Council (ALW) partly supported the investigations with financial aid from the Netherlands Organization for Scientific Research (NWO). The constructive comments of the reviewers greatly improved the current version of this paper.

References

[1] Baldocchi DD, Vogel CA, Hall B. Seasonal variation of energy and water vapour exchange rates above and below a boreal jack pine forest canopy. J Geophys Res Atmos 1997;02:28939–51.
[2] Black TA, Kelliher FM. Processes controlling understorey evapotranspiration. Phil Trans Roy Soc London B 1989;324:207–31.
[3] Dekker SC, Bouten W, Schaap MG. Analysing forest transpiration model errors with artificial neural networks. J Hydrol 2001;246:197–208.
[4] Efron B, Tibshirani RJ. An introduction to the bootstrap. Monographs on statistics and applied probability. New York: Chapman & Hall; 1993.
[5] FAO/UNESCO. Soil map of the world, revised legend. World soil resources report 1988;60:1–138.
[6] Falge E, Graber W, Siegwolf E, Tenhunen JD. A model of the gas exchange response of Picea abies to habitat conditions. Trees 1996;10:277–87.
[7] Goudriaan J. Crop mircrometeorology: a simulation study. PUDOC 1977, Centre for Agricultural publishing and documentation, Wageningen, The Netherlands.
[8] Heimovaara TJ, Bouten W. A computer controlled 36-channel time domain reflectometry system for monitoring soil water contents. Water Resour Res 1990;36:2311–6.
[9] Huntingford C, Cox PM. Use of statistical and neural network techniques to detect how stomatal conductance responds to changes in the local environment. Ecol Model 1997;97:217–46.
[10] Jarvis PG. The interpretation of the variations in leaf water potential and stomatal conductance found in canopies in the field. Philos Trans Roy Soc London B 1976;273:593–610.
[11] Jarvis PG. Scaling processes and problems. Plant Cell Environ 1995;18:1079–89.
[12] Kelliher FM, Leuning R, Schulze ED. Evaporation and canopy characteristics of coniferous forests and grasslands. Oecologia 1993;95:153–63.
[13] Kelliher FM, Lloyd J, Arneth A, Byers JN, Seveny TMc, Milukova I, et al. Evaporation from a central siberian pine forest. J Hydrol 1998;205:279–96.
[14] Lamaud E, Ogeé J, Brunet Y, Berbigier P. Validation of eddy flux measurements above the understorey of a Pine forest. Agri Forest Meteorol 2001;106(3):187–203.
[15] Landsberg JJ, Kaufmann MR, Binckley D, Isebrands J, Jarvis PG. Evaluating progress toward closed forest models based on fluxes of carbon, water and nutrients. Tree Physiol 1991;9:1–15.
[16] Lee X, Black TA. Atmospheric turbulence within and above a Douglas-fir stand. Part II: Eddy fluxes of sensible heat and water vapour. Boundary Layer Meteorol 1993;64(4):369–89.
[17] Lockwood JG. The sensitivity of the water balance of a wet multilayer model pine canopy to variations in micrometeorological input. Climate Change 1992;20:23–56.
[18] Loustau D, Cochard H. Utulisation d'une chambre de transpiration portable pour l'estimation de l'évapotranspiration d'un sous-bois de pin maritime á molinie. Sci Ann For 1991;48:29–45.
[19] Marquardt DW. An algorithm for least-squares estimation of non-linear parameters. SIAM J Appl Math 1963;11:431–41.
[20] Moore CJ. Frequency response corrections for eddy correlation systems. Boundary Layer Meteorol 1986;37:17–35.
[21] Musters PAD, Bouten W. Assessing rooting depths of an Austrian pine stand by inverse modelling soil water content maps. Water Resour Res 1999;35(10):3041–8.
[22] Musters PAD, Bouten W, Verstraten JM. Potentials and limitations of modelling vertical distributions of root water uptake of an Austrian pine forest on a sandy soil. Hydrol Processes 2000;14(1):103–15.
[23] Nielsen RH. Neurocomputing. USA: Addition-Wesley Publishing Company; 1991.
[24] Priestly CHB, Taylor RJ. On the assessment of surface flux and evaporation using large-scale parameters. Month Weather Rev 1972;100:81–92.
[25] Roberts JS, Wallace JS, Pitman RM. Factors affecting stomatal conductance of bracken below a forest canopy. J Appl Ecol 1984;21:643–55.
[26] Sajikumar N, Thandaveswara BS. A non-linear rainfall-runoff model using an artificial neural network. J Hydrol 1999;216:32–55.

[27] Schaap MG, Bouten W. Modeling soil water retention curves of sandy soils using neural networks. Water Resour Res 1996;32:3033–40.
[28] Schaap MG, Leij F, Van Genuchten MTh. Neural network analysis for hierarchical prediction of soil hydraulic properties. Soil Sci Soc Amer J 1998;62:847–55.
[29] Schelde K, Kelliher FM, Massman WJ, Jensen KH. Estimating sensible and latent heat fluxes from a temperate broad-leaved forest using the Simple Biosphere (SiB) model. Agri Forest Meteorol 1997;84:285–95.
[30] Sellers PJ, Shuttleworth WJ, Dolman JL. Calibrating the simple biosphere model for Amazonian tropical forest using field and remote sensing data. Part I: Average calibration with field data. J Appl Meteorol 1989;28:727–59.
[31] Shuttleworth WJ, Wallace JS. Evaporation from sparse crops – an energy combination theory. Quart J Roy Meteorol Soc 1985;111:839–55.
[32] Shuttleworth WJ, Gurney RJ. The theoretical relationship between foliage temperature and canopy resistance in sparse crops. Quart J Roy Meteorol Soc 1990;116:497–519.
[33] Stewart JB. Modelling surface conductance of pine forest. Agri Forest Meteorol 1988;43:19–35.
[34] Van Wijk MT, Bouten W. Water and carbon fluxes above European coniferous forests modelled with artificial neural networks. Ecol Model 1999;120(2–3):181–97.
[35] Wang YP, Jarvis PG. Description and validation of an array model – MAESTRO. Agri Forest Meteorol 1990;51: 257–80.
[36] Webb EK, Pearman GI, Leuning R. Corrections of flux measurements for density effects due to heat and water vapour transfer. Q J Meteorol Soc 1980;106:85–100.